Aberrant Wnt signalling induces comedo-like changes in the upper hair follicle

Wei Shang
Institute of Medical Biology/Skin Research Institute of Singapore, Agency for Science, Technology, and Research https://orcid.org/0000-0002-5936-5974

Alvin Tan
Institute of Medical Biology/Skin Research Institute of Singapore, Agency for Science, Technology, and Research

Maurice Steensel
Skin Research Institute of Singapore

Xinhong Lim (xinhong.lim@ntu.edu.sg)
Skin Research Institute of Singapore

Article

Keywords: Wnt signals, comedonal acne, hair follicle

Posted Date: October 7th, 2020

DOI: https://doi.org/10.21203/rs.3.rs-84554/v1

Version of Record: A version of this preprint was published at Journal of Investigative Dermatology on December 17th, 2021. See the published version at https://doi.org/10.1016/j.jid.2021.11.034.

Aberrant Wnt signalling induces comedo-like changes in the upper hair follicle

Shang Wei[1], Alvin Yong Quan Tan[1], Maurice A.M. van Steensel[1,2]* and Xinhong Lim[1,2]*

1. Institute of Medical Biology/Skin Research Institute of Singapore, Agency for Science, Technology, and Research;
2. Lee Kong Chian School of Medicine, Nanyang Technological University Singapore

Correspondence and requests for materials should be addressed to:
Xinhong Lim (xinhong.lim@ntu.edu.sg)
Maurice van Steensel (maurice_vansteensel@ntu.edu.sg)
*Both authors contributed equally to this work

Abstract

Comedonal acne is a common skin disease characterized by cystic dilation of the hair follicle junctional zone. While the molecular mechanisms of acne pathogenesis are not well understood, an emerging hypothesis holds that imbalances in key signalling pathways may lead to abnormal fate determination of sebaceous progenitor cells. The subsequent accumulation of cells could then cause cyst formation in the hair follicle junctional zone and lower infundibulum, forming blackheads. This notion is supported by the observation that 2,3,7,8-tetrachlorodibenzo-p-dioxin (TCDD) causes severe comedonic acne and seboatrophy by inducing fate changes in *Lrig1*-expressing stem cells, as well as recent human GWAS studies implicating the Wnt signalling pathway in acne. To test the possible involvement of Wnt signals in blackhead formation, we used an Lrig1-CreERT2 mouse line to modulate Wnt signalling in stem cells of the junctional zone, which are known to contribute to the junctional zone, infundibulum, and sebaceous glands. We find that persistent activation of Wnt signalling in the junctional zone leads to formation of comedone-like cysts with associated atrophic sebaceous glands. The cysts strongly express stem cell markers and can be partially reduced by treatment with all-*trans* retinoic acid, a well-established acne treatment, as well as by inhibition of Hedgehog signalling. In contrast, loss of Wnt signalling leads to enlargement of the junctional zone, infundibulum and sebaceous glands. These data lead us to suggest that abnormal Wnt signalling could be involved in acne pathogenesis by inhibiting differentiation and retaining junctional zone cells in a proliferative progenitor state, leading to their accumulation into comedones.

Introduction

The highly prevalent skin disease acne vulgaris[1,2] is characterized by the development of comedones (blackheads and whiteheads) as well as inflammatory skin lesions. The disorder is usually self-limiting but can leave disfiguring scars and is associated with a considerable psychosocial and economic burden. With more than 90 percent of the world population affected at some point in their lives, acne represents an important public health problem[3] . Unfortunately, the most effective treatments available come with significant disadvantages. Antibiotic use in acne is contributing to antimicrobial resistance, whereas retinoids (synthetic vitamin A analogues) cause skin irritation when used topically and are highly teratogenic when administered systemically. Alternatives are needed, but their development has been hampered by a lack of insight into the mechanisms underlying acne pathogenesis.

Acne comedones are cystic structures within the junctional zone (JZ) of hair follicles. The JZ, or lower infundibulum, is where sebaceous glands, which secrete lipids in the form of sebum, connect to the hair follicle (HF) via a short, keratinized duct. Comedones are currently thought to be formed by abnormal differentiation and proliferation of cells in the JZ[4–7]. In support of this notion, comedo-associated sebaceous glands (SGs) are atrophic[8], implying they are no longer being replenished by their progenitor cells. It is known that, in the mouse, a stem cell pool in the JZ maintains itself, in addition to the SG and infundibulum[9,10]. Therefore, one hypothesis proposed for acne pathogenesis is that imbalances in key signalling pathways may alter the fate of JZ residing stem cells, promoting the growth of the junctional zone in lieu of that of the SG[8] . This hypothesis is supported by studies of 2,3,7,8-tetrachlorodibenzo-p-dioxin (TCDD), a compound that causes severe comedonic acne with complete disappearance of sebaceous glands[11]. TCDD strongly induces CYP1A1 in humans[11], and in mice[12], it was subsequently found that *Lrig1*-expressing JZ stem cells were the first to exhibit a CYP1A1 response to TCDD exposure, which prevented their differentiation into sebocytes and led to seboatrophy[12]. This suggests that abnormal differentiation of JZ stem cells in humans may similarly result in their accumulation and subsequent cyst formation, manifesting as a comedo. In further support of the involvement of JZ stem cells in acne pathogenesis, a recent GWAS study has identified a loss-of-function variant in *WNT10A*[13], a key stem cell signal, as protective from acne. Accordingly, a gain-of-function variant appeared to be the most prominent risk factor in the population that was analysed. Consistent with these human data, conditional deletion of *Wnt10a* in mice results in enlarged sebaceous glands[14]. In addition, *Lgr6,* which marks several progenitor cell populations in the pilosebaceous unit (PSU), was also found to be associated with acne susceptibility.

While Wnt is one of the key signals that influence lineage specification by stem cells in the epidermis and its appendages[15–17], how it works in the upper hair follicle specifically remains incompletely understood. There is apparently conflicting evidence for the role of Wnt signaling in the upper hair follicle, as inhibiting Wnt in *Krt14*$^{+ve}$ cells using different transgenes (dominant-negative *Lef1* and *Tcf3*)[18,19] has been reported to both promote sebaceous tumors and cause loss of sebaceous glands. One potential reason for this is that these studies are confounded by the overly broad targeting of Wnt signalling in all of the epidermal stem and progenitor cells (which express *Krt14*), and the results are compound phenotypes that aggregate the effects of Wnt manipulation in multiple epidermal stem cell pools. Consistent with this, recent studies have shown that activating β-catenin in individual epidermal stem cell pools marked by *Lrig1*, *Lgr6* and *Lgr5* respectively[10], induces distinct tumor types, suggesting that it is important to study the impact of modulating key stem cell signals such as Wnt in specific epidermal compartments.

To test the hypothesis that fate imbalances in JZ stem cells cause cyst formation, we set out to modulate cell fate signalling in this population, which is known to express *Lrig1*[19,20]. We used Lrig1-CreERT2 mice[20] to perform conditional gain/loss-of-function studies of Wnt signalling of *Lrig1*-expressing stem cells residing in the JZ. We found that Wnt activation via the deletion of *Apc* inhibits sebaceous differentiation of JZ stem cells and promotes their proliferation, resulting in cyst formation within the JZ as well as atrophic sebaceous glands. In contrast, Wnt inhibition via deletion of β-catenin stimulates differentiation to infundibulum, JZ and sebaceous lineages with retention of mostly normal architecture.

Materials and Methods

Experimental Animals

Lrig1-CreERT2 (018418), β-catenin$^{\Delta ex2\text{-}6\text{-}flox/flox}$(004152) and Rosa26-mTmG (007676) mice have been described previously and were obtained from The Jackson Laboratory. APC^{580S} mice were a gift from Dr. Nick Barker, IMB, A*STAR. All experiments were performed on postnatal day 45 (P45) animals, with treatments topically applied on the dorsal.

Lrig1-CreERT2/Rosa26-mTmG mice were topically treated with a single dose of 1.5mg of 4-hydroxytamoxifen (4-OHT) [Sigma, H6278] in acetone for lineage tracing. *Lrig1*-CreERT2/β-catenin$^{\Delta ex2\text{-}6\text{-}flox/flox}$, *Lrig1*-CreERT2/Rosa26-mTmG/β-catenin$^{\Delta ex2\text{-}6\text{-}flox/flox}$, *Lrig1*-CreERT2/*APC*^{580S}

and *Lrig1*-CreERT2/Rosa26-mTmG/*APC*^{580S} mice were treated with a single dose of 1.5mg of 4-OHT in acetone for knockout experiments. For pharmacological treatment experiments, *Lrig1*-CreERT2/*APC*^{580S} mice were induced by single topical application on the dorsal region of 1.5mg 4-OHT in acetone. At day 5 post 4-OHT, 1% of the Smoothened antagonist TAK-441 [Active Biochem, A1172] or 0.1% all-*trans*-retinoic acid [Sigma, R2625] dissolved in vehicle (70% propylene glycol [Sigma, W294004], 20% DMSO [Sigma, D2650], 10% ethanol) was topically applied on the dorsal region daily until day 11 post 4-OHT, at which point the mice were sacrificed for tissue harvest.

All experimental procedures were approved by A*STAR Animal Care and Use Committee (IACUC 151053), and NTU Institutional Animal Care and Use Committee (AUP19020 and AUP18107) and were performed according to Singapore Bioethics Council guidelines.

Histology and Immunofluorescence

Animals were sacrificed and dorsal skins harvested. For paraffin blocks, tissues were fixed in 4% paraformaldehyde (PFA) [Life Technologies, Cat no. 28906] for 20-24h at room temperature (22-24°C) with shaking. Tissues were washed in phosphate buffered saline (PBS) and dehydrated through a series of ethanol (30%, 50%, 70%), followed by xylene and paraffin wax embedding. Paraffin sections of 6-10μm thicknesses were obtained using Leica RM2255 microtome (Leica Microsystems). Sections were dewaxed, rehydrated, counterstained with Hematoxylin [Thermofisher, Cat no. 7231] and Eosin [Sigma, Cat no. E6003] dehydrated and mounted using Cytoseal (Thermo Scientific, Cat no. 48212-154).

For cryoblock processing, tissues were fixed in 4% PFA for 20-24h at room temperature (22-24°C) with shaking. Tissues were washed in PBS and stored in 30% sucrose (w/v) at 4°C overnight. Tissues were embedded in OCT medium [Tissue-Tek] and cryoblocks were stored at -80°C. Frozen sections of 8-10μm and 200μm thickness were obtained using CM3050S cryostat [Leica Microsystems]. Sections of 8-10μm thickness were washed in PBS, incubated in blocking buffer (2% normal goat serum [Jackson ImmunoResearch, Cat no. 005-000-121] and 0.2% Triton X in PBS) for 1h at room temperature (22-24°C), followed by incubation with primary antibody diluted in blocking buffer at 4°C overnight. Sections were then incubated with secondary antibody diluted in blocking buffer for 1h at room temperature and were mounted in ProLong Diamond antifade mountant with DAPI [Life Technologies, Cat no. P36962]. All washes in between incubations were performed using PBS.

The following antibodies were used: Rabbit monoclonal Ki67 SP6 (1:200) [abcam, Cat no.ab16667], Rabbit monoclonal anti-Beta-catenin E247 (1:200) [abcam, Cat no. ab32572],

Rabbit polyclonal anti-Filaggrin Poly19058 (1:500) [Biolegend, Cat no. 905801], Goat polyclonal anti-LRIG1 Alexa Fluor 488-conjugated (1:50) [R&D Systems, Cat no. FAB3688G], and Goat anti-Rabbit Alexa Fluor 488/568/647-conjugated (1:200) [Life Technologies, Cat no. A11034/A11036/A32733]. The following dye was used: Phalloidin Alexa Fluor 568 (1:250) [Life Technologies, Cat no. A12380].

RNA in Situ Hybridization

Tissues sections were cut at 6µm thickness, air-dried at room temperature (22-24°C) and processed for RNA *in-situ* detection by using RNAscope 2.5HD Red assay and RNAscope 2.5HD Duplex assay [Advance Cell Diagnostics, Cat no. 322350 & 322500] according to the manufacturer's protocols. Frozen sections at 10µm thickness were processed for RNA *in-situ* hybridization using RNAscope Fluorescent Multiplex assay [Advance Cell Diagnostics, Cat no. 320850] according to manufacturer's protocols. The following RNAscope probes were used for detection: *Lrig1* (NM_008377), *Axin2* (NM_015732), *Axin2* (NM_004655), *APC* (NM_007462), *c-Myc* (NM_001177354), *Lgr6* (NM_001033409), *Shh* (NM_009170), *Ihh* (NM_010544), *Dhh* (NM_007857), *Smo* (NM_176996), *Ptch1* (NM_008957), *Gli1* (NM_010296), *Dkk1* (NM_010051), *Dkk4* (NM_145592), *Lgr5* (NM_010195), *Krt79* (NM_146063), *Wls* (NM_026582), *Wnt3* (NM_009521), *Wnt6* (NM_009526), *Wnt7b* (NM_009528), *Polr2a* (positive control), *DapB* (negative control).

Quantification of Sebaceous Gland Volume and Infundibulum Dimensions

Frozen tissue sections of 200µm thickness were washed in PBS to obtain tissue strips from the OCT medium. These strips were incubated in 0.5% Saponin containing Proteinase K (20µg /mL) [Thermofisher, Cat no. EO0491] for 1h at room temperature (22-24°C), washed in 0.5% Saponin, then incubated in 0.5% Saponin containing Phalloidin Alexa Fluor 568 (1:200), HCS LipidTOX Green/DeepRed neutral lipid stain (1:1000) [Life Technologies, Cat no. H34475/H34477] and DAPI [Life Technologies, Cat no. R37606] at 4°C overnight with shaking. Tissue strips were then incubated in RapiClear 1.49 [Sunjin Lab] at 4°C overnight, transferred onto an iSpacer (0.2mm) [Sunjin Lab] on a slide, mounted with RapiClear and used for imaging.

Z-stack images of pilosebaceous units were obtained using an Olympus FV3000RS Inverted Confocal microscope equipped with 30x silicone oil objectives at 22-24°C. Images were processed in IMARIS software version 9.20 [Oxford Instruments], using Surface and Filament functions to obtain various quantification measurements: a) Sebaceous gland volume (μm^3) b) Cell layer width (µm) at upper and lower infundibulum, c) Maximum diameter (µm) of

infundibulum and d) Length (μm) of infundibulum. These measurements were used to calculate the mean average ± SEM from two to /three mice per condition.

Microscopic Imaging

Histological and RNA in-situ sections were imaged by using Zeiss AxioImager and Nikon ECLIPSE Ts2R microscope. Immunofluorescent sections were imaged using a Zeiss LSM510 and Olympus FV3000RS Inverted Confocal Microscope. Image acquisitions were done at room temperature (22-24°C) using 10x, 20x and 40x oil objectives. Image processing was performed using Fiji (Fiji is Just ImageJ) software version 2.0.0 written by Wayne Rasband.

Statistical Analysis

Quantification data measurements were plotted and analysed on Prism 8 software version 8.1.2. Statistical analysis was performed using the unpaired Mann-Whitney test. P values of less than 0.05 were considered statistically significant.

Results

Modulation of Wnt signalling results in contrasting upper hair follicle and sebaceous gland phenotypes

We first confirmed *Lrig1* expression in the JZ of telogen-phase dorsal hair follicles using three different methods: *Lrig1* RNA in situ hybridization (Fig.1A), immunofluorescence staining for Lrig1 protein expression (Fig.1B) and short-term genetic lineage tracing using *Lrig1-CreERT2-mTmG* mice (2 days, Fig.1C and D). The labelled cells expanded from the JZ into the infundibulum and sebaceous gland for up to 4 weeks after the initial pulse of 4-OHT (Fig.1D), confirming that they are self-renewing JZ stem cells with the ability to differentiate into infundibulum and sebaceous gland daughter cells[9,10].

We next tested the effects of either activating or ablating Wnt signalling conditionally in the JZ, by crossing *Lrig1-CreERT2* mice with APC^{580s}[21,22] and β-catenin flox[23,24] mice respectively to generate gain-of-function (*Lrig1-Apc*) and loss-of-function models (*Lrig1-βcat*) (Fig.1E and F). Both APC and β-catenin are key components of the Wnt signalling pathway and are widely expressed in the pilosebaceous units. β-catenin transduces Wnt signalling by migrating from the cytoplasm to the nucleus upon binding of Wnt ligands to their receptors[25,26], while APC negatively regulates Wnt signalling by degrading β-catenin.

Adult control and *Lrig1-Apc* mutant mice were topically treated with a single dose of 4-OHT at P45 and examined 2, 5, 7 and 11 days later (Fig.1E and F). *Lrig1-Apc* mice had to be sacrificed by 11 days following 4-OHT application, as the *Apc* deletion resulted in lethal intestinal dysfunction with expanded crypts (Supplementary Figure S1), consistent with the known intestinal expression of *Lrig1*[16] and previous studies[21,27] . The dorsal skin in both control and mutant mice remained in telogen phase until the end of the experiments and no visible fur phenotypes were observed. This suggests that the lower portion of the HF was not affected and is consistent with the observation that *Lrig1-CreERT2* had little to no expression in the bulge under such condition.

Following the induction of *Apc* deletion, hair follicles (HFs) in *Lrig1-Apc* mutant dorsal skin began to dilate at the JZ at Day 7 (Fig.1G), coinciding with upregulated *Axin2* expression, which is a reliable indicator of Wnt activity (Supplementary Figure S2). This progressed to the formation of massive cysts in the JZ that strongly expressed *Axin2* at Day 11. The cysts appeared morphologically to be mostly confined to the JZ, as the thickness of the infundibulum did not differ significantly from that in controls (Fig.1G and I). The lower HF, including the hair bulge, of mutant animals was unaffected (Fig.1G) but their sebaceous glands were significantly smaller, with a mean volume of $0.62*10^5$ μm^3 compared to $0.89*10^5$ μm^3 in controls (Fig.1G and I, $p < 0.001$) at the time of examination.

In contrast to *Lrig1-Apc* mice, *Lrig1-βcat* mice developed an elongated and hyperplastic infundibulum and junctional zone (Fig.1H) within four weeks of induction. The sebaceous glands were twice the size in mutants as compared to controls, with a mean volume of $1.6*10^5$ μm^3 versus $0.8*10^5$ μm^3 (Fig.1H and J). Similar to *Lrig1-Apc* mice, the bulge and cycling lower portion of the HF (hair bulb)[28] of *Lrig1-βcat* mice were unaffected.

Cell proliferation is generally confined to basal cells of the various epidermal compartments[29] , which is consistent with what we observed in control skin immunostained for Ki67, a well-established cell proliferation marker (Fig.2A). *Lrig1-Apc* mouse HFs had greatly increased numbers of $Ki67^+$ cells in multiple layers of the JZ cysts (arrows in Fig.2A), suggesting that the phenotype arises from cells confined to the JZ compartment. In comparison, *Lrig1-βcat* mice also had increased $Ki67^+$ cells, but these were more evenly distributed throughout the infundibulum/JZ and sebaceous gland (arrowheads in Fig.2A, quantification in Supplementary Figure S3).

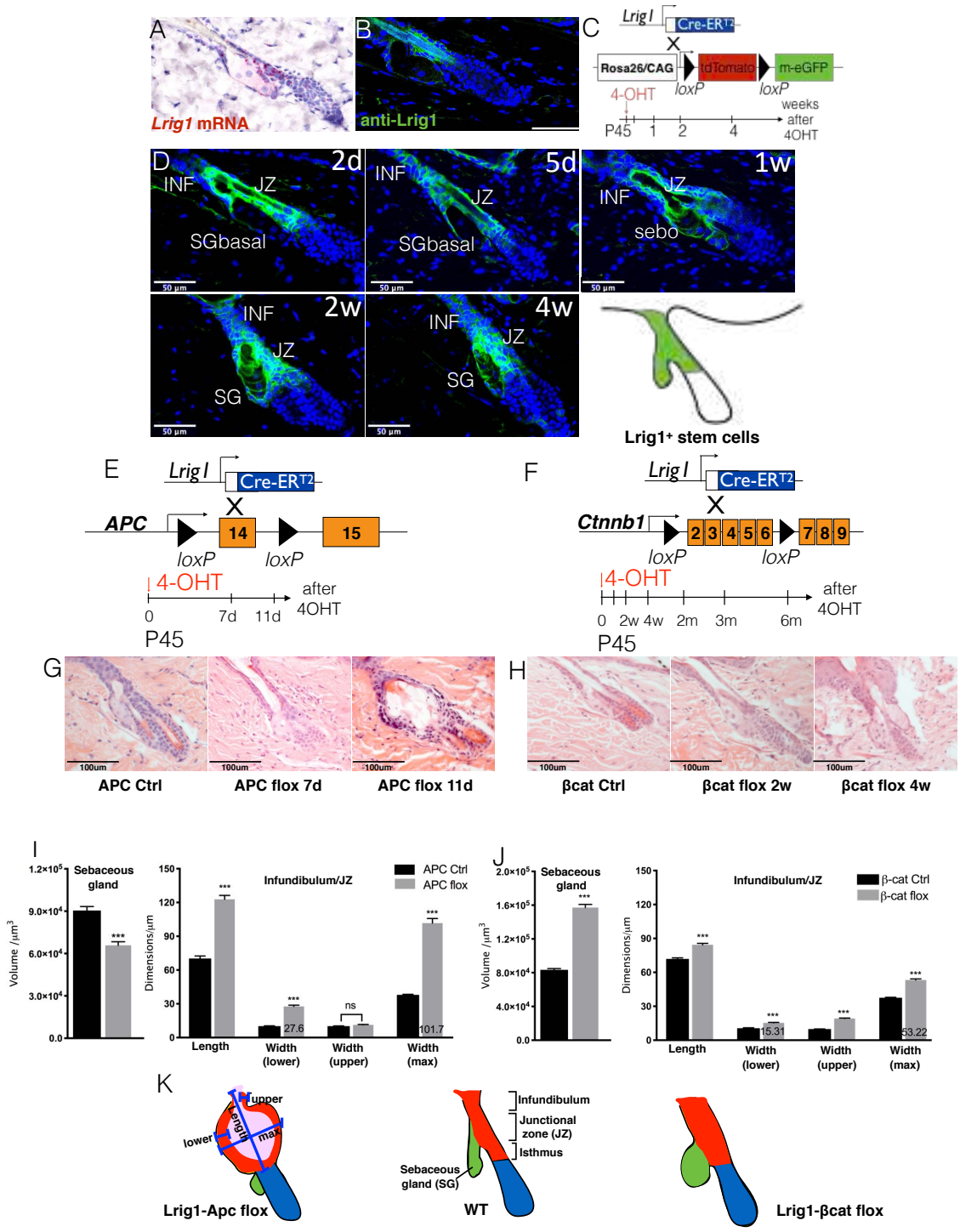

Figure 1. Modulation of Wnt signalling results in contrasting upper hair follicle phenotypes

(A and B) RNA *in situ* hybridization (A) and immunofluorescense (B) of *Lrig1* in adult mouse dorsal skin (P45). Skin tissue sections were counterstained with DAPI to label nuclei (blue). (C) Schematic representation of the genetic elements for *Lrig1* lineage tracing during adult homeostasis and the experimental setup. (D) Dorsal skin tissues of *Lrig1-CreERT2/Rosa26-mTmG* mice collected 2 days, 5days, 1 week, 2 weeks and 4 weeks after 4-OHT treatment at P45, counterstained with DAPI to label nuclei (blue), red fluorescence of membrane tdTomato was not shown. JZ, junctional zone; INF, infundibulum; SG, sebaceous gland; SGbasal, basal cells of sebaceous gland; sebo, differentiated sebocytes. Scale bars, 50 µm. (E and F) Schematic representation of the genetic elements for *Apc*

deletion (E) and *Ctnnb1* deletion (F) and experimental setups. (G) H&E stained sections of dorsal skin from *Lrig1-Apc* mutant and control mice (APC Ctrl) 7 days and 11 days after 4-OHT treatment. (H) H&E stained sections of dorsal skin from *Lrig1-βcat* mutant and control mice (*βcat* Ctrl) 2 weeks and 4 weeks after 4-OHT treatment. (I and J) Quantifications of infundibulum/junctional zone dimensions and the sebaceous glands volumes (indicated by lipidTOX staining in green). Length, measurement from IFE to the point of SG duct connecting to the HFs; Width (lower), thickness of cell layers in the junctional zone; Width (upper), thickness of the cell layers in the infundibulum; Width (max), maximum diameters of the JZ cysts. N=60-180 imaged hair follicles from 2-5 mice in each group, respectively. N=110-290 sebaceous glands from 2-5 mice. Data are mean±SEM. ***p<0.001. (K) Schematic of phenotype development in *Lrig1-Apc* (11 days) and *Lrig1-βcat* (4 weeks) mutants.

Wnt-activated JZ cysts contain large numbers of cells expressing stem cell marker *Lgr6* and *Lgr5*

While β-catenin was mostly localized at the plasma membrane of cells in control epidermis, *Lrig1-Apc* mutant cysts presented with strongly increased overall levels as well as nuclear localization of β-catenin (Fig.2B). This suggested strong upregulation of Wnt signalling in the cysts, confirmed by greatly increased *Axin2* expression (Fig. 2C). Consistent with these data and the increased proliferation observed, the Wnt target gene *c-Myc* was also strongly and uniformly expressed in the *Lrig1-Apc* cysts. In addition, *Wls* and Wnt ligands that are expressed in the upper HFs (*Wnt3, 6, 7b*) were also upregulated (Supplementary Figure S4D-G).

As expected, β-catenin was completely depleted in the hyperplastic JZ, infundibulum and enlarged SGs of the *Lrig1-βcat* mice, demonstrating effective deletion in JZ stem cells that was passed on to daughter cells in those compartments (Fig.2B). Consistent with this, *Axin2* showed clearly reduced expression in the upper HF of *Lrig1-βcat* mutant mice (Fig.2C).

Lgr6, a Wnt signalling pathway mediator and stem cell marker, is expressed in hair follicle isthmus stem cells that give rise to HFs, SGs and IFE[12]. In *Lrig1-Apc skin*, *Lgr6* was strongly upregulated in the basal cells of the junctional zone cysts, while its expression did not change appreciably in *Lrig1-βcat* mutant skin (Fig.2E). *Lgr5*, which marks stem cells in the hair bulge and has likewise been reported as a Wnt target gene, is not typically expressed in the JZ. Its expression was also increased in the *Lrig1-Apc* cysts, whereas it was not changed in *Lrig1-βcat* mutant (Fig.2E).

These data suggest that increased Wnt signalling is sufficient to promote the proliferation of cells with stem cell characteristics that remain in the JZ and form cysts, whereas the loss of Wnt activity promotes the differentiation of JZ cells to the infundibulum, isthmus and SG cell lineages, while retaining an intact HF architecture.

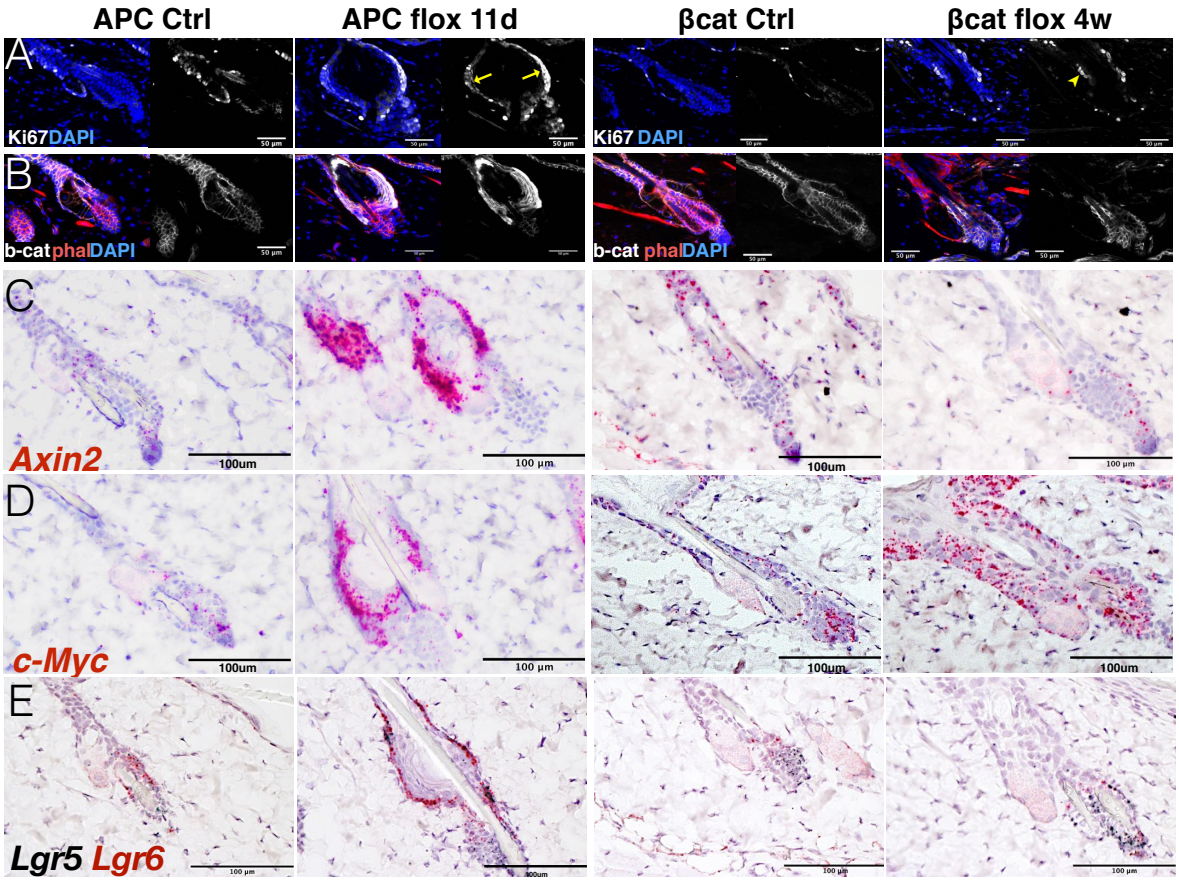

Figure 2. Wnt-hyperactivated JZ cysts contain large numbers of cells expressing *Lgr6* and *Lgr5*
(A and B) Immunolabeled with the Ki-67 (A) and b-catenin (B) antibodies, and counterstained with phalloidin to label F-actin (red) or with DAPI to label nuclei (blue). Single color images for *β*-catenin and Ki-67 are shown in gray scale. Arrows and arrowhead indicate Ki67^{+ve} cells in *Lrig1-Apc* cyst and *Lrig1-βcat* JZ, respectively. Scale bars, 50 μm.(C-E) Representative images of RNA *in situ* hybridization for Wnt targeted genes: *Axin2* (C), *c-Myc* (D), *Lgr6* and *Lgr5* (E) as performed on *Lrig1-Apc* and *Lrig1- βcat* mutants and controls. Scale bars, 100 μm.

Contributions of *Lrig1*$^{+ve}$ stem cells upon deletion of *Apc* or *Ctnnb1*

To determine if the modulation of Wnt signalling indeed affects the movement and contribution of *Lrig1*$^{+ve}$ stem cells to the upper PSU lineages, we created conditional mutant lineage tracing mice by breeding *Lrig1-CreERT2* mice with APC^{580S}- or β-catenin flox mice carrying the Rosa26-mTmG reporter (*Lrig1-Apc-mTmG* and *Lrig1-βcat-mTmG*) (Fig.3A). Adult mice were pulsed with a single topical application of 4-OHT at P45 (Fig.3B). Lineage tracing revealed that at Day11 in *Lrig1-Apc-mTmG* mutant mice, mGFP^{+ve} cells remained mostly restricted to the JZ cyst and contributed less to SGs than was the case in controls (Fig 3C). One explanation for this was that some basal cells of SGs were labelled and differentiated into sebocytes by Day 7 but did not get replenished from the JZ cells, causing the drop in labelled sebocytes from Day 7

to 11. Consistent with this interpretation, we observed high *Axin2* expression in the basal cells of JZ cysts and low *Axin2* expression in the differentiated sebocytes in *Lrig1-Apc-mTmG* mutant skin, suggesting that Wnt-activated *Lrig1-APC-mTmG* mutant cells were confined to the JZ cysts (Supplementary Figure S5). In contrast, mGFP^{+ve} stem cells that had lost β-catenin contributed extensively to the entire upper PSU, including the elongated INF, JZ and enlarged SG (Fig.3D). Taken together, these data suggest that Wnt signalling maintains JZ cells in a proliferative stem cell state, and loss of Wnt signalling drives fate commitment and differentiation toward the specified cell lineages (Fig.3E).

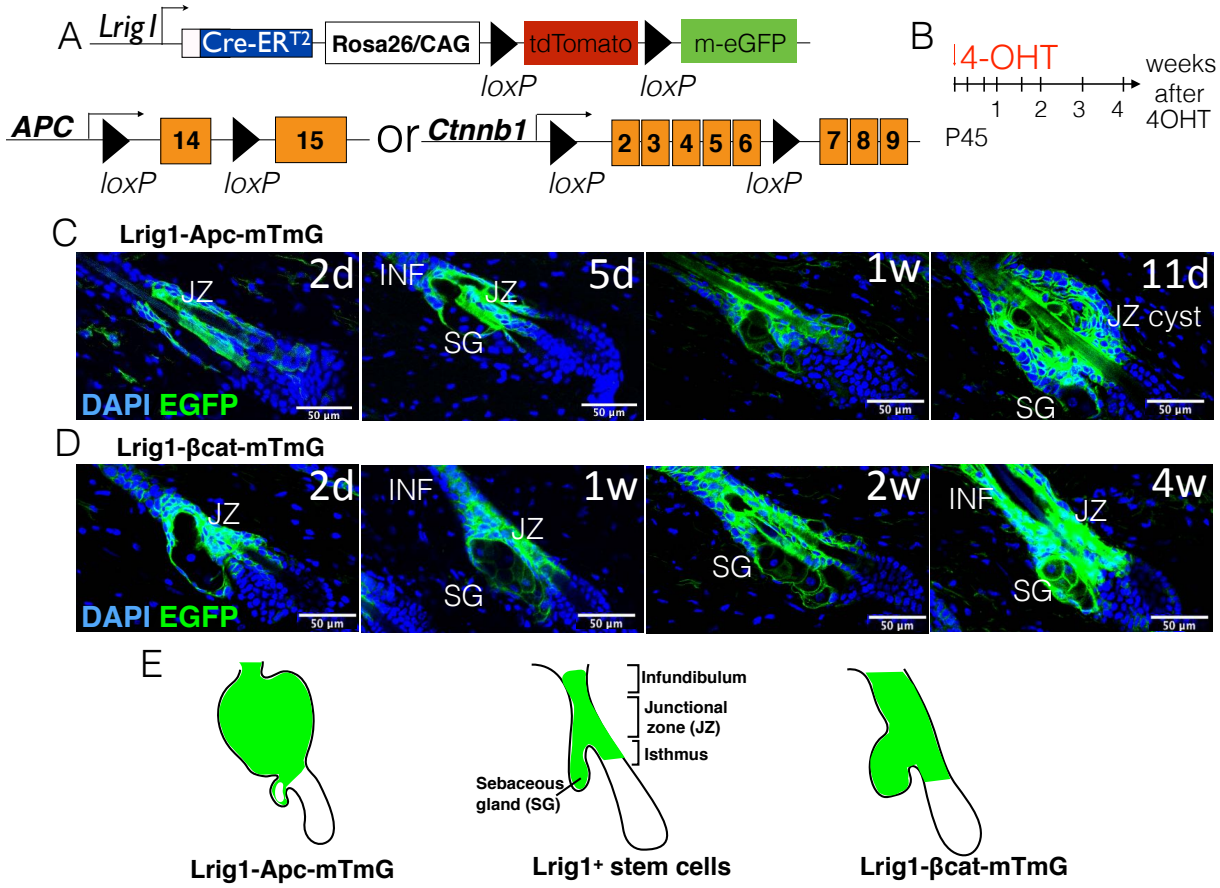

Figure 3. Contributions of *Lrig1*$^{+ve}$ stem cells when *Apc* or *Ctnnb1* was deleted
(A and B) Schematic representation of the genetic elements for lineage tracing (A) and experimental setups (B). (C and D) Dorsal skins collected at serial time points as indicated after 4-OHT treatment and stained with DAPI. Red fluorescence of membrane tdTomato was not shown. Scale bars, 50 μm. (E) Schematic of *Lrig1*$^{+ve}$ stem cells contributions to upper HFs when *Apc* or *Ctnnb1* was ablated.

Hedgehog signalling drives *Lrig1-Apc* JZ cyst formation

We next asked what other signalling pathways might mediate the effects of Wnt-induced cyst formation. Given that Sonic hedgehog (*Shh*) is a well-known target of canonical Wnt signalling

in the skin[30] and has been implicated in SG homeostasis[31], we examined Hedgehog ligand expressions in the skins of mutant mice with upregulated/ablated Wnt signalling as well as their controls. Consistent with previous studies, there was little to no detectable Hedgehog ligand RNA expression in control mouse telogen phase skin[32,33], though there was clear expression of Hedgehog target genes *Gli1* and *Patched1* (*Ptch1)*, suggesting that there is active Hedgehog signalling[34] and that the Hedgehog ligands may be expressed elsewhere in the skin or body and transported to the epidermis[35]. In mutant *Lrig1-Apc* skins however, *Shh* ligand expression was strongly induced in the upper HFs at Day 7 (Supplementary Figure S2) and was highly enriched in the basal cells of the JZ cyst at Day 11 (Fig.4A). There was little to no *Ihh* and *Dhh* expression in either mutant or control mice (Fig.4B and C). Expression of *Smoothened (Smo)*, which encodes the Hedgehog signalling transducer, was also increased in the *Lrig1-Apc* JZ cyst, consistent with the known ability of Wnt signalling to upregulate *Smo* expression[36]. Expression of *Ptch1* and *Gli1* was both markedly increased (Fig.4D) compared to controls, indicating strong activation of Hedgehog signalling in the *Lrig1-Apc* JZ cysts (Fig.4E and F). Of note, this upregulation was largely restricted to the outermost basal layer of the JZ cyst, despite the overall increase of *Axin2* and *Shh* expression (Supplementary Figure S6), implying that Hedgehog signalling was not activated in the inner layers. No changes in Hedgehog ligands and pathway target genes were detected in *Lrig1-βcat* mutants (Fig.4).

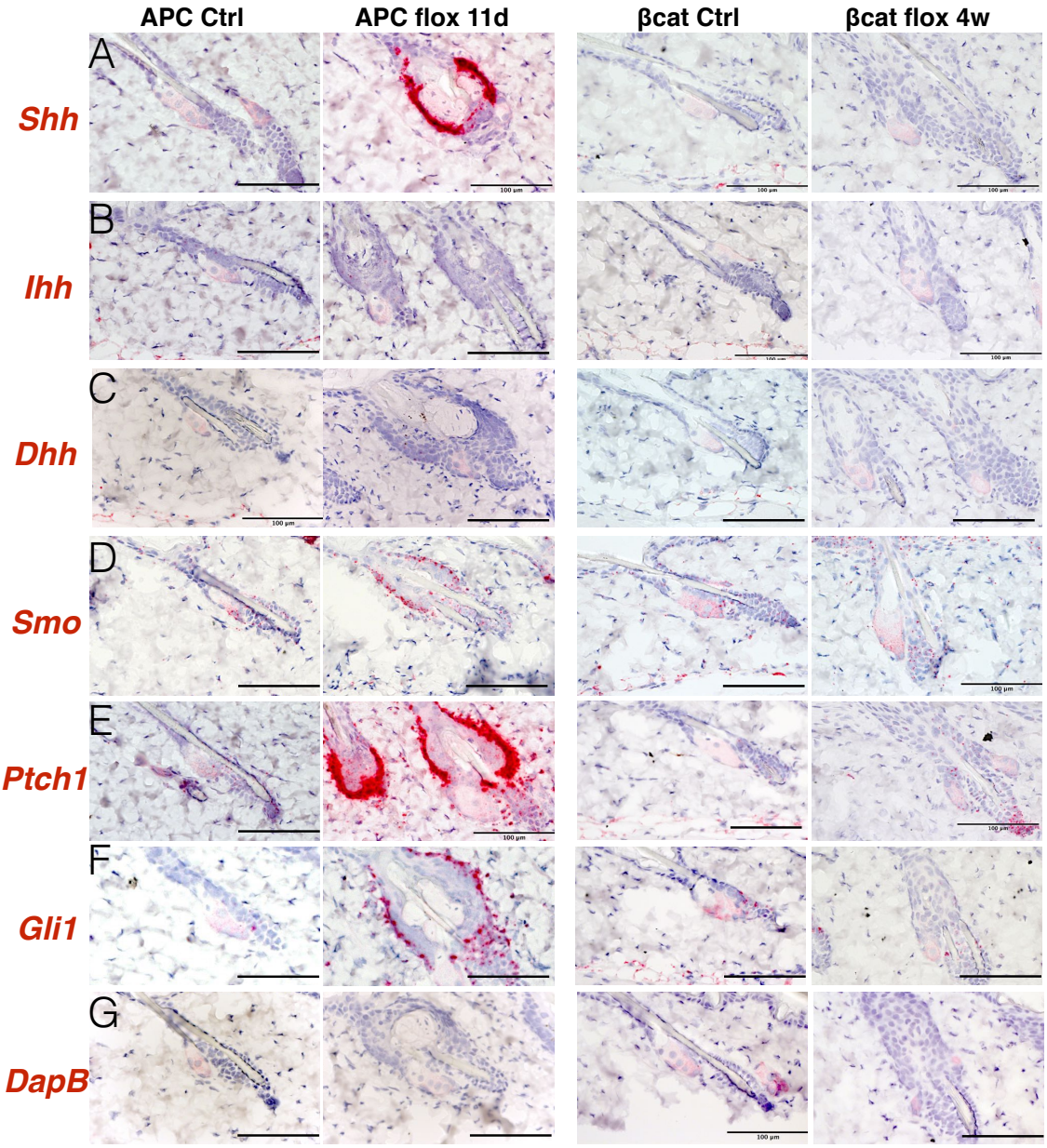

Figure 4. Hedgehog signalling was upregulated in APC loss/Wnt activation induced JZ cyst, but not *Ctnnb1* loss-induced expansions

(A-G) RNA *in situ* hybridization of genes in Hedgehog signaling pathways in *Lrig1-Apc* (11 days) and *Lrig1-βcat cat* (4 weeks) mutants and controls. *Shh*, Sonic hedgehog; *Ihh*, Indian hedgehog; *Dhh*, Desert hedgehog; *Smo*, smoothened; *DapB*, negative control. Scale bars, 100μm.

These observations suggest that upregulated Wnt signalling activates Shh ligand production and the Hedgehog signalling cascade, which may lead to JZ cyst formation. To test this, we topically applied the small molecule Smoothened antagonist TAK-441 in a single daily dose to *Lrig1-Apc* mice dorsal skin. The mean elimination half-life of TAK-441 is 13.5 to 22.6 hours[37], hence a single daily dose should suffice to inhibit Smoothened activity throughout the treatment period. We treated the animals for 5 days following 4-OHT treatment until tissue harvest at Day

11 (Fig.5A). TAK-441 treatment showed a minor effect on the HF of control mice comparing to the vehicle treated ones, in the length of the upper HF, the width of the JZ and the maximum diameter (Fig.5B and C). In mutant animals however, TAK-441 treatment significantly reduced the number/ thickness of the cell layers and the maximum diameter of the cysts. However, there seemed to be no effect on the length of the upper PSU (Fig.5C). TAK-441 treatment did not affect *Axin2* and *Shh* expression levels in mutant JZ cysts compared to untreated cysts, but moderately decreased *Smo* expression and greatly reduced *Ptch1 and Gli1* expression (Fig.5D). In addition, *Lgr6* expression was much lower in the treated group than the vehicles, reflective of the delayed phenotype development. These data provide functional evidence that Wnt-induced cyst formation is mediated at least in part by Shh signalling.

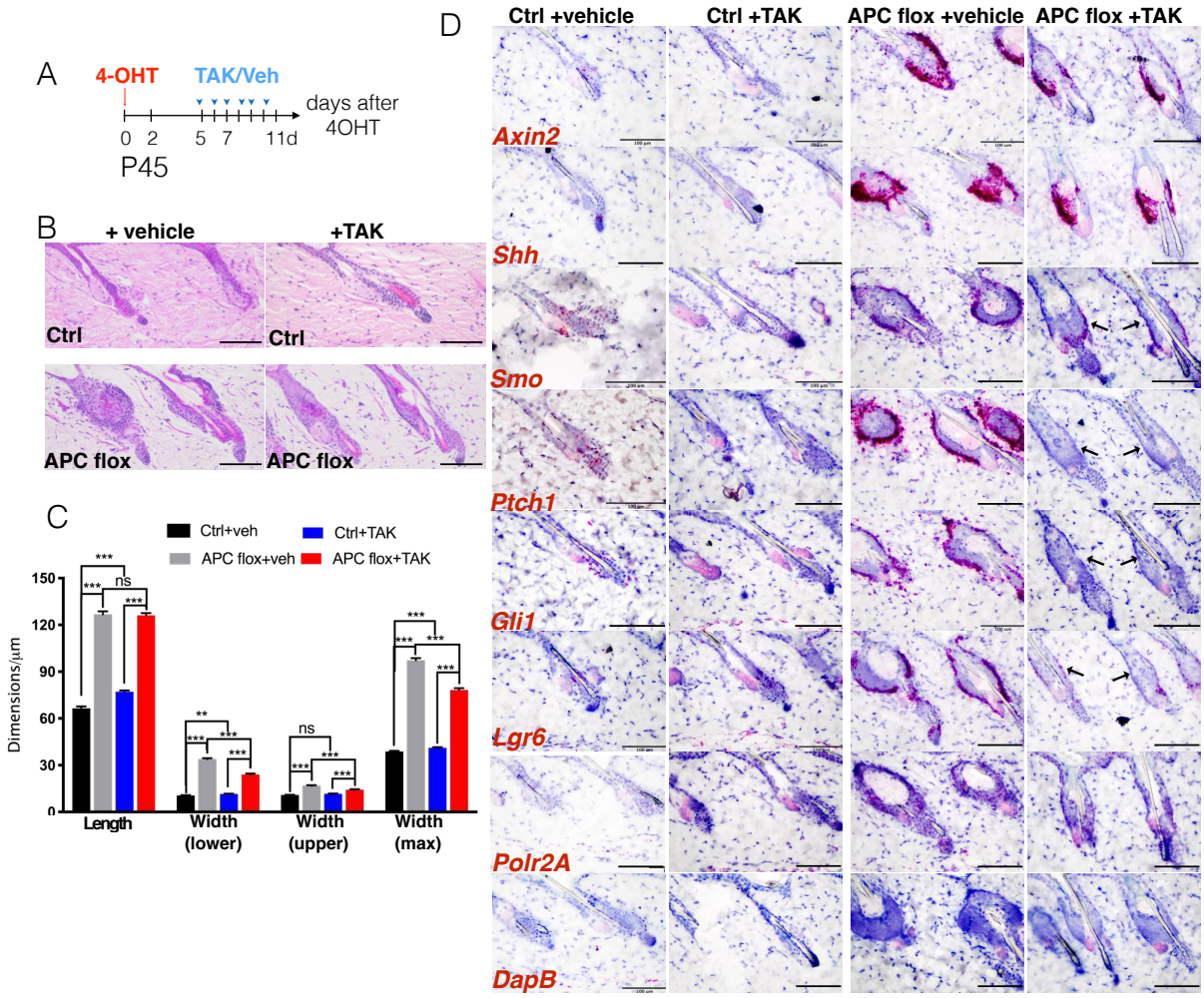

Figure 5. APC loss/Wnt activation induced cyst formation is Hedgehog signaling-dependent. (A) Experimental setup. Mice were topically treated with 4-OHT at P45 and subsequently with 1% TAK-441 single dose daily from P50 till tissue harvest. (B) H&E staining of dorsal skin sections from *Lrig1-Apc* mutant and controls treated with vehicles or TAK-441. Scale bars, 50µm. (C) Quantifications of infundibulum/junctional zone dimensions and the sebaceous glands volumes of *Lrig1-Apc* mutant and controls treated with vehicles or TAK-441. N=153-184 imaged hair follicles from 2-3 mice in each group, respectively. Data are mean±SEM. ***p<0.001. (D) RNA *in situ* hybridization of *Axin2, Shh*, Smoothened,

Ptch1, Gli1 and *Lgr6* in *Lrig1-Apc* mutant and controls treated with vehicles or TAK-441. *DapB*, negative control; *Polr2A*, positive control. Scale bars, 100 μm.

All-trans retinoic acid rescues the *Lrig1-Apc* mice phenotype

Given the resemblance of the *Lrig1-Apc* JZ cysts to comedones, we next asked if established acne treatments might ameliorate the *Lrig1-Apc* phenotype. *All-trans* retinoic acid (atRA) is a metabolite of vitamin A_1 and widely used in the treatment of both comedonic and inflammatory acne as an initial and maintenance treatment[38]. atRA is also known to antagonize Wnt and Hedgehog signalling in embryonic stem cells[39], possibly through induction of the secreted Wnt antagonist *Dkk-1*[40]. We topically treated the dorsal skin of control and *Lrig1-Apc* mutant mice with 0.1% atRA starting 5 days post 4-OHT application and assessed the skin at Day 11 (Fig.6A). Consistent with previously reported observations in mouse[41], topical treatment with atRA caused visibly dry and scaly skins in both *Lrig1-Apc* control and mutant mice (Fig.6B). These visible abnormalities were not seen in vehicle-treated animals (data not shown).

AtRA-treated *Lrig1-Apc* mutants had reduced dilation of the upper HFs and smaller cysts as compared to the vehicle-treated mutant mice (Fig.6C). This indicates that atRA was able to, at least partially, reduce or delay the Wnt activation-induced development of JZ cysts. Consistent with this, atRA treatment reduced *Axin2* and *Lgr6* expression as well as nuclear β-catenin in *Lrig1-Apc* mutant JZ cysts, while simultaneously strongly inducing *Dkk4* in the JZ and SG (Fig 6D, Supplementary Figure 7). In addition, expression of *Shh* ligand, *Gli1* and *Ptch1* were also decreased (Supplementary Figure S8). These data suggest that atRA may reduce comedo-like JZ cysts through the dual inhibition of hedgehog signalling and Wnt signalling at the level of β-catenin. While it is unlikely to be acting at the Wnt ligand level in these *Lrig1-Apc* animals, the data lead us to speculate that atRA could limit comedogenesis in acne through *Dkk4* induction with normal β-catenin degrading complex.

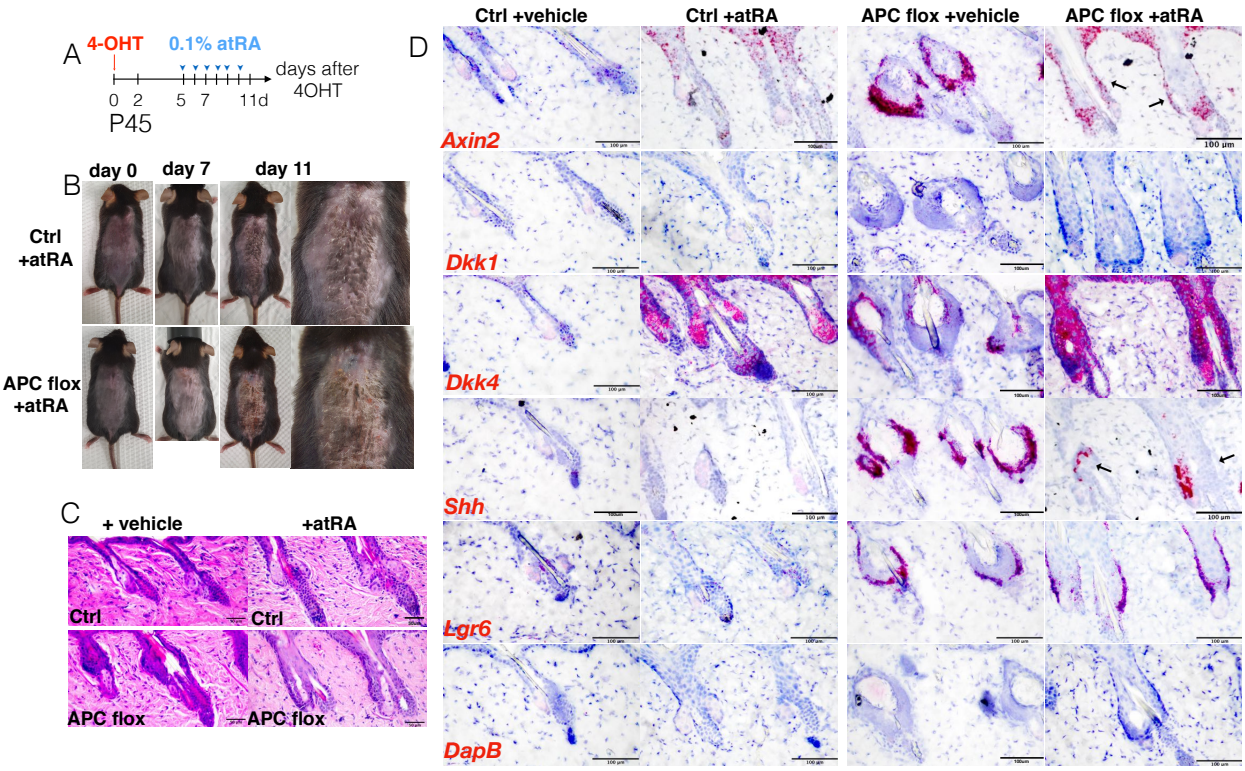

Figure 6. All-*trans* Retinoic acid rescued *Lrig1-Apc* mice phenotypes
(A) Experimental setup. Mice were topically treated with 4-OHT at P45 and subsequently with 0.1% all-*trans*-Retinoic acid (atRA) single dose daily from P50 till tissue harvest. (B) Representative pictures of shaved and treated *Lrig1-Apc* mutant and control mice skin changes with 0.1% atRA applications.(C) H&E staining of dorsal skin sections from *Lrig1-Apc* mutant and controls treated with vehicles or atRA. Scale bars, 50μm. (D) RNA *in situ* hybridization of *Axin2, Dkk1, Dkk4, Shh, Lgr6* and *DapB* in *Lrig1-Apc* mutant and controls treated with vehicles or atRA. Scale bars, 100 μm.

Discussion

In this study, we modulated Wnt/β-catenin signalling in the HF JZ using mouse models, to test the hypothesis that imbalances in stem cell signals lead to abnormal fate determination that could manifest in upper hair follicle pathologies, such as acne comedones. We show that loss of Wnt signalling in the HF JZ leads to enlargement of the JZ, INF and SGs. In contrast, gain-of-function of Wnt signalling leads to cyst formation in the JZ with atrophy of associated SGs, leaving the lower portion of HF unaffected.

How does Wnt signalling promote JZ stem cell fate? Our data suggests that this may occur at least in part by potentiation of autocrine Wnt signalling. *Lrig1-Apc* JZ cysts showed strong upregulation of the isthmus stem cell marker[42,43] and Wnt target gene[44] *Lgr6* in the JZ basal cells. LGR6 is a high affinity receptor for R-spondin, which potentiates Wnt signalling, and *Lgr6*

can induce stemness (e.g. of ovarian cancer cells[45], colorectal cancer cells[46]) by enhancing Wnt/β-catenin signalling. This considered, our data here could be taken to suggest that active Wnt signalling may set up autocrine signalling loops that reinforce the stem cell identity in the JZ. This suggests that the cells accumulating in the *Lrig1-Apc* cysts may be stem cells and explains why the associated SGs appear to atrophy, since they are no longer being replenished by JZ stem cells.

We further identify additional transcription factors that cooperate with β-catenin to determine cell fates. We examined *c-Myc,* whose identity as a Wnt target gene is well established in colon[47], but for which there is conflicting evidence regarding whether or not it is similarly so in the skin[14]. Our observation that *c-Myc* expression is upregulated in both gain- and loss-of-function conditions is in line with this inconsistency. One interpretation of this data is that *c-Myc* responds in a non-monotonic fashion to Wnt signalling. "Just right" levels of Wnt signalling through β-catenin may generally actually constrain *c-Myc* expression in *Lrig1*$^{+ve}$ cells, serving to control proliferation. This is consistent with the previous study showing that β-catenin is not required for proliferation[48] and with our observation that cell proliferation was increased in *Lrig1-βcat* mutant skin (Fig.2 and Fig.S3). Alternatively, even though *c-Myc* is upregulated in both increased and ablated Wnt signalling conditions, there could be different cofactors and multiple regulatory pathways in each signalling scenario that change the cellular responses and, hence, the resulting phenotype[49] .

We further demonstrated that Shh signalling is at least in part driving the *Lrig1-Apc* JZ cysts formation and that Smoothened inhibitor effectively reduced the phenotype development. How might Shh signalling affect compartment specification in the pilosebaceous units? Contradictory evidence exists for the role of Shh in the JZ and SG compartments. It has previously been shown that enhanced activation of Shh signalling in keratinocytes leads to the formation of hyperplastic or ectopic sebaceous glands[50,51], either by expressing a constitutively activated form of the hedgehog signalling effector *Smo* or overexpressing *Gli2* driven by *K5*. However, Hedgehog activation induced by *Ptch1* ablation in *Lrig1*$^{+ve}$ cells leads to HF-associated BCC-like tumor arising from infundibulum and the associated SGs appears shrunken rather than expanded[52]. This latter finding is more consistent with our results and suggests that the differences with the *K5*-driven phenotype may be the result of confounding contributions from non-*Lrig1*$^{+ve}$ compartments in the *K5* pool. While we did not observe tumors in the present study, we cannot rule out the possibility that continued activation of Wnt (and thus Hedgehog) signalling might lead to tumor formation.

While our approach of conditionally activating Wnt signalling in the upper hair follicle using *Lrig1-CreERT2* mice has similarities to the studies performed by Kreztchmar and colleagues[10], it differs in several important ways: (1) we used different *Lrig1-CreERT2* mice and conditional Wnt-activating alleles (*Apc* vs *Ctnnb1* delta exon-3); (2) phenotypes in our mice developed quickly, with JZ cyst formation in our *Lrig1-Apc* mutants developing within 11 days, compared to the 4-6 weeks tumor development time in their model; and (3) the phenotypes were histologically different, with our *Lrig1-Apc* mice developing dilation of the JZ and the formation of cysts that resembled acne comedones, whereas Kreztchmar and colleagues reported solid growths that more closely resembled human trichoadenomas [53]. These differences may have resulted from different deletion efficiencies in the different *Lrig1-Cre* lines that our two groups used, or from distinct responses of *Lrig1*$^{+ve}$ cells to β-catenin stabilization versus *Apc* deletion. β-catenin has other roles not directly related to Wnt signalling (*e.g.,* regulation and coordination of cell–cell adhesion) and APC performs several roles related to Wnt signalling outside of its classically defined scaffolding function in the β-catenin destruction complex. For example, its interaction with nuclear β-catenin leads to repression of Wnt target genes through facilitating β-catenin's nuclear export[54]. As such, deletion of *Apc* could result in stronger upregulation of Wnt signalling than β-catenin stabilization, and this could have caused much more rapid cyst formation. We cannot exclude that more prolonged Wnt activation in the *Lrig1*$^{+ve}$ cells may induce the *Lrig1-Apc* mutant cysts to transition from being like comedones to being more like trichoadenomas, but this is not a possibility that we could test in our system.

This study has several limitations that could be addressed in future research. First, while we targeted Wnt signalling in *Lrig1*$^{+ve}$ stem cells that are mostly confined to the junctional zone, we also detected *Lrig1* expression in the basal layer of the SGs and hair bulge (Fig.1A). Since the associated SGs were shrunken with low *Axin2* expression in *Lrig1-Apc* mutant, we believe that it is unlikely that the *Lrig1*$^{+ve}$ SGs basal cells contribute to the JZ cyst phenotype. While we cannot fully exclude a contribution of *Lrig1*$^{+ve}$ bulge stem cells to the JZ cyst formation, previous lineage tracing studies have shown that the bulge and JZ are regulated and populated independently during homeostasis. As such, we believe that the phenotype we observe is likely to be mostly the result of fate specification of JZ stem cells to infundibulum rather than bulge. Second, we chose to use *Apc* deletion over β-catenin to activate Wnt signalling because of the potentially confounding role of β-catenin in cell adhesion. APC is a crucial component of the β-catenin degradation complex and deletion of *Apc* is very commonly performed to activate Wnt signalling in well-established epithelial stem cell systems (e.g. intestine). We cannot exclude that APC could also be involved in β-catenin-independent processes that may contribute to the phenotypes we have observed[55], and this is a general limitation shared with other Wnt gain-of-function mutants that are currently available. For example, APC deficiency leads to YAP

activation[56] which is known to promote cell proliferation, independently of β-catenin complex. However, evidence showing that Wnt activation in *Lrig1*$^{+ve}$ cells leads to infundibular growth supports the central role of Wnt signalling in fate determination in this compartment.

While Wnt signalling pathway is unquestionably a major determinant in cell specification, whether it is involved in comedone pathogenesis has not yet been tested. We detected *AXIN2* expression in comedones using in situ hybridization, suggesting active Wnt signalling there (Supplementary Figure S10) and supporting a potential role for it in acne comedogenesis. In mouse, JZ cysts arising in *Lrig1-Apc* mutant skin resemble acne comedones both histologically and in their ability to respond to known acne treatments. Just like acne comedones that present with massive follicular dilation filled with keratin (or skin debris) [36] (Supplementary Figure 10) and increased filaggrin expression[57], *Lrig1-Apc* JZ cysts are lined by proliferative cells, highly express filaggrin (Supplementary Figure S9) and contain cellular debris. They are also associated with atrophic SGs. The well-established acne treatment, atRA, ameliorates these comedo-like *Lrig1-Apc* JZ cysts, by inhibiting Wnt and Shh signalling. Existing animal models for studying acne, such as the Mexican hairless dog, Rhino mouse and rabbit ear assay are used for assessing retinoids or other topical reagents but do not closely mimic the human disease[58]. Our data suggest that the *Lrig1-Apc* model may be a more accurate experimental model of comedogenesis. While there is, to the best of our knowledge, no evidence for *Apc* mutations in human comedones formation, our data reveal a crucial role for Wnt and the downstream Shh signaling in regulating JZ cells specification, with faulty instructions resulting in comedone-like growths. Hence, we suggest that Wnt and Shh signalling might constitute molecular targets for acne interventions.

Acknowledgements

We thank the following colleagues who have supported and provided valuable edits to the manuscript: Dr Keith Tan, and Dr Beng Hui Lim. We thank Dr Nicholas Barker for discussions and for donating APC^{580s} mice. This work was supported by the Agency for Science, Technology, and Research in Singapore Acne and Sebaceous Gland IAF-PP (H17/ H17/01/a0/008).

Author Contributions

S.W. performed the experiments, data analysis and the writing of this paper. A.Y.Q.T performed experiments, data analysis and participated in scientific discussions. M.v.S and X.L. contributed to the overall project direction, data interpretation, discussion and writing of this paper.

Competing interests

We declare no competing interests.

References

1. Smithard, A., Glazebrook, C. & Williams, H. C. Acne prevalence, knowledge about acne and psychological morbidity in mid-adolescence: A community-based study. *Br. J. Dermatol.* (2001). doi:10.1046/j.1365-2133.2001.04346.x
2. Tan, H. H., Tan, A. W. H., Barkham, T., Yan, X. Y. & Zhu, M. Community-based study of acne vulgaris in adolescents in Singapore. *Br. J. Dermatol.* (2007). doi:10.1111/j.1365-2133.2007.08087.x
3. Semyonov, L. Acne as a public health problem. *Ital. J. Public Health* **7**, 112–114 (2010).
4. Saurat, J. H. Strategic Targets in Acne: The Comedone Switch in Question. *Dermatology* (2015). doi:10.1159/000382031
5. Clayton, R. W. *et al.* Homeostasis of the sebaceous gland and mechanisms of acne pathogenesis. *Br. J. Dermatol.* 1–14 (2019). doi:10.1111/bjd.17981
6. Knutson, D. D. Ultrastructural observations in acne vulgaris: the normal sebaceous follicle and acne lesions. *J. Invest. Dermatol.* (1974). doi:10.1111/1523-1747.ep12676804
7. Hughes, B. R., Morris, C., Cunliffe, W. J. & Leigh, I. M. Keratin expression in pilosebaceous epithelia in truncal skin of acne patients. *Br. J. Dermatol.* (1996). doi:10.1111/j.1365-2133.1996.tb07609.x
8. Kligman, A. M. An overview of acne. *J. Invest. Dermatol.* (1974). doi:10.1111/1523-1747.ep12676801
9. Page, M. E., Lombard, P., Ng, F., Göttgens, B. & Jensen, K. B. The epidermis comprises autonomous compartments maintained by distinct stem cell populations. *Cell Stem Cell* **13**, 471–82 (2013).
10. Kretzschmar, K. Compartmentalized Epidermal Activation of b-catenin differentially affects lineage reprogramming and underlies tumor heterogeneity (sup). *Cell Rep.* **14**, 1–8 (2016).
11. Saurat, J. H. *et al.* The cutaneous lesions of dioxin exposure: Lessons from the poisoning of Victor Yushchenko. *Toxicol. Sci.* (2012). doi:10.1093/toxsci/kfr223
12. Fontao, F., Barnes, L., Kaya, G., Saurat, J. H. & Sorg, O. High susceptibility of Lrig1 sebaceous stem cells to TCDD in mice. *Toxicol. Sci.* **160**, 230–243 (2017).
13. Petridis, C. *et al.* Genome-wide meta-analysis implicates mediators of hair follicle development and morphogenesis in risk for severe acne. *Nat. Commun.* **9**, (2018).
14. Xu, M. *et al.* WNT10A mutation causes ectodermal dysplasia by impairing progenitor cell proliferation and KLF4-mediated differentiation. *Nat. Commun.* **8**, 15397 (2017).
15. Millar, S. E. Molecular mechanisms regulating hair follicle development. *J. Invest. Dermatol.* **118**, 216–25 (2002).
16. Tinkle, C. L., Pasolli, H. A., Stokes, N. & Fuchs, E. New insights into cadherin function in epidermal sheet formation and maintenance of tissue integrity. *Proc Natl Acad Sci U S A* **105**, 15405–15410 (2008).
17. Xinhong Lim, R. N. Wnt Signaling in Skin Development ,. *Cold Spring Harb. Perspect. Biol.* (2013).
18. Niemann, C., Owens, D. M., Hülsken, J., Birchmeier, W. & Wat, F. M. Expression of ΔNLef1 in mouse epidermis results in differentiation of hair follicles into squamous

epidermal cysts and formation of skin tumours. *Development* **129**, 95–109 (2002).
19. Nguyen, H., Rendl, M. & Fuchs, E. Tcf3 Governs Stem Cell Features and Represses Cell Fate Determination in Skin. *Cell* (2006). doi:10.1016/j.cell.2006.07.036
20. Powell, A. E. *et al.* The pan-ErbB negative regulator, Lrig1, is an intestinal stem cell marker that functions as a tumor suppressor. *Cell* **149**, 146–158 (2013).
21. Barker, N. *et al.* Crypt stem cells as the cells-of-origin of intestinal cancer. *Nature* **457**, 608–611 (2009).
22. Shibata, H. *et al.* Rapid colorectal adenoma formation initiated by conditional targeting of the APC gene. *Science (80-.).* (1997). doi:10.1126/science.278.5335.120
23. Lim, X. *et al.* Interfollicular epidermal stem cells self-renew via autocrine Wnt signaling. *Science* **342**, 1226–30 (2013).
24. Brault, V. *et al.* Inactivation of the beta-catenin gene by Wnt1-Cre-mediated deletion results in dramatic brain malformation and failure of craniofacial development. *Development* (2001).
25. Clevers, H. & Nusse, R. Wnt/β-catenin signaling and disease. *Cell* **149**, 1192–205 (2012).
26. Lang, C. M. R., Chan, C. K., Veltri, A. & Lien, W. H. Wnt signaling pathways in Keratinocyte carcinomas. *Cancers (Basel).* **11**, (2019).
27. Powell, A. E. *et al.* Inducible loss of one Apc allele in Lrig1-expressing progenitor cells results in multiple distal colonic tumors with features of familial adenomatous polyposis. 16–23 (2014). doi:10.1152/ajpgi.00358.2013
28. Erdoğan, B. Anatomy and Physiology of Hair. in *Hair and Scalp Disorders* (2017). doi:10.5772/67269
29. Owens, D. M. & Watt, F. M. Contribution of stem cells and differentiated cells to epidermal tumours. *Nat. Rev. Cancer* **3**, 444–451 (2003).
30. Huelsken, J., Vogel, R., Erdmann, B., Cotsarelis, G. & Birchmeier, W. beta-Catenin controls hair follicle morphogenesis and stem cell differentiation in the skin. *Cell* **105**, 533–545 (2001).
31. Niemann, C. & Horsley, V. Development and homeostasis of the sebaceous gland. *Semin. Cell Dev. Biol.* **23**, 928–36 (2012).
32. Hsu, Ya-Chieh; Li Lishi; Fuchs, E. Transit-Amplifying Cells Orchestrate Stem Cell Activity and Tissue Regeneration. **157**, 935–949 (2014).
33. Avigad Laron, E., Aamar, E. & Enshell-Seijffers, D. The Mesenchymal Niche of the Hair Follicle Induces Regeneration by Releasing Primed Progenitors from Inhibitory Effects of Quiescent Stem Cells. *Cell Rep.* **24**, 909-921.e3 (2018).
34. Abe, Y. & Tanaka, N. Roles of the Hedgehog Signaling Pathway in Epidermal and Hair Follicle Development, Homeostasis, and Cancer. *J. Dev. Biol.* **5**, 12 (2017).
35. Brownell, I., Guevara, E., Bai, C. B., Loomis, C. A. & Joyner, A. L. Nerve-derived sonic hedgehog defines a niche for hair follicle stem cells capable of becoming epidermal stem cells. *Cell Stem Cell* **8**, 552–565 (2011).
36. Wang, Y., Lin, P., Wang, Q., Zheng, M. & Pang, L. Wnt3a-regulated TCF4/β-catenin complex directly activates the key Hedgehog signalling genes Smo and Gli1. *Exp. Ther. Med.* **16**, 2101–2107 (2018).
37. Goldman, J. *et al.* Phase I dose-escalation trial of the oral investigational Hedgehog signaling pathway inhibitor TAK-441 in patients with advanced solid tumors. *Clin. Cancer Res.* **21**, 1002–1009 (2015).
38. Williams, H. C., Dellavalle, R. P. & Garner, S. Acne vulgaris. *Lancet* **379**, 361–72 (2012).
39. Osei-Sarfo, K. & Gudas, L. J. Retinoic acid suppresses the canonical Wnt signaling pathway in embryonic stem cells and activates the noncanonical Wnt signaling pathway. *Stem Cells* (2014). doi:10.1002/stem.1706
40. Verani, R. *et al.* Expression of the Wnt inhibitor Dickkopf-1 is required for the induction of neural markers in mouse embryonic stem cells differentiating in response to retinoic acid. *J. Neurochem.* (2007). doi:10.1111/j.1471-4159.2006.04207.x
41. Gericke, J. *et al.* Regulation of Retinoid-Mediated Signaling Involved in Skin Homeostasis by RAR and RXR Agonists/Antagonists in Mouse Skin. *PLoS One* **8**, (2013).
42. Snippert, H. J. *et al.* Lgr6 marks stem cells in the hair follicle that generate all cell

lineages of the skin. *Science (80-.).* **327**, 1385–1389 (2010).
43. Barker, N., Bartfeld, S. & Clevers, H. Tissue-resident adult stem cell populations of rapidly self-renewing organs. *Cell Stem Cell* **7**, 656–70 (2010).
44. Lien, W.-H. *et al.* In vivo transcriptional governance of hair follicle stem cells by canonical Wnt regulators. *Nat. Cell Biol.* **16**, 179–190 (2014).
45. Ruan, X. *et al.* Silencing LGR6 Attenuates Stemness and Chemoresistance via Inhibiting Wnt/β-Catenin Signaling in Ovarian Cancer. *Mol. Ther. - Oncolytics* **14**, 94–106 (2019).
46. Wang, F. *et al.* Downregulation of Lgr6 inhibits proliferation and invasion and increases apoptosis in human colorectal cancer. *Int. J. Mol. Med.* (2018). doi:10.3892/ijmm.2018.3633
47. He, T. *et al.* Identification of c- MYC as a Target of the APC Pathway. *Science (80-.).* **281**, 1509–1512 (1998).
48. Posthaus, H. *et al.* β-Catenin is not required for proliferation and differentiation of epidemal mouse keratinocytes. *J. Cell Sci.* **115**, 4587–4595 (2002).
49. Cottle, D. L. *et al.* c-MYC-induced sebaceous gland differentiation is controlled by an androgen receptor/p53 axis. *Cell Rep.* **3**, 427–41 (2013).
50. Allen, M. *et al.* Hedgehog Signaling Regulates Sebaceous Gland Development. *Am. J. Pathol.* **163**, 2173–2178 (2003).
51. Gu, L.-H. & Coulombe, P. a. Hedgehog signaling, keratin 6 induction, and sebaceous gland morphogenesis: implications for pachyonychia congenita and related conditions. *Am. J. Pathol.* **173**, 752–61 (2008).
52. Peterson, S. C. *et al.* Basal cell carcinoma preferentially arises from stem cells within hair follicle and mechanosensory niches. *Cell Stem Cell* **16**, 400–412 (2015).
53. Ho, J. & Bhawan, J. Folliculosebaceous neoplasms: A review of clinical and histological features. *J. Dermatol.* **44**, 259–278 (2017).
54. Hamada, F. & Bienz, M. The APC tumor suppressor binds to C-terminal binding protein to divert nuclear beta-catenin from TCF. *Dev. Cell* **7**, 677–685 (2004).
55. Magnani. Identification of Endogenous Adenomatous Polyposis Coli Interaction Partners and β-Catenin-Independent Targets by Proteomics. *Physiol. Behav.* **176**, 139–148 (2018).
56. Cai, J., Maitra, A., Anders, R. A., Taketo, M. M. & Pan, D. β -Catenin destruction complex- independent regulation of Hippo – YAP signaling by APC in intestinal tumorigenesis. 1493–1506 (2015). doi:10.1101/gad.264515.115.
57. Kurokawa, I., Mayer-da-Silva, A., Gollnick, H. & Orfanos, C. E. Monoclonal antibody labeling for cytokeratins and filaggrin in the human pilosebaceous unit of normal, seborrhoeic and acne skin. *J. Invest. Dermatol.* **91**, 566–571 (1988).
58. Jang, Y. H., Lee, K. C., Lee, S., Kim, D. W. & Lee, W. J. HR-1 Mice : A New Inflammatory Acne Mouse Model. **27**, 257–264 (2015).

Figures

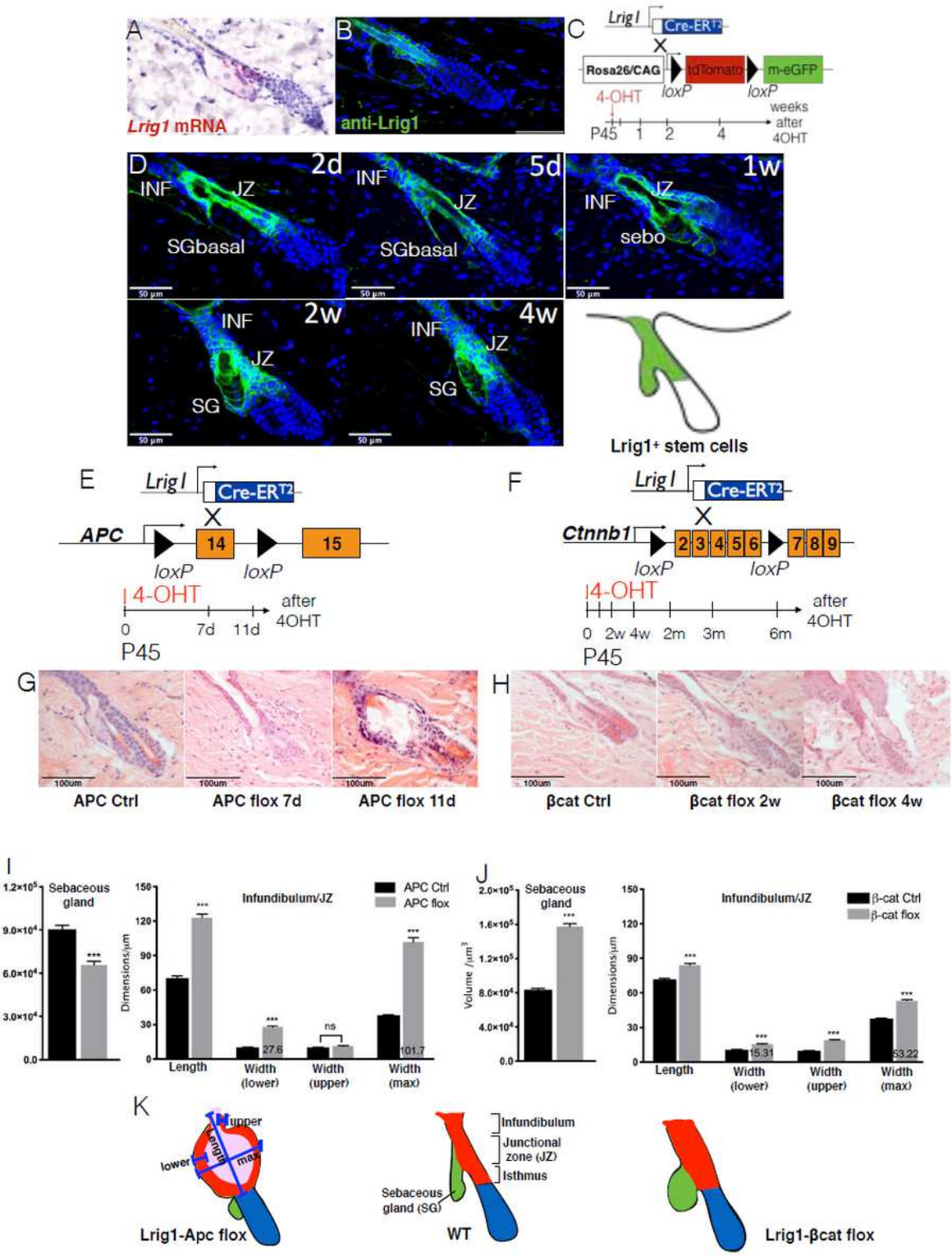

Figure 1

Modulation of Wnt signalling results in contrasting upper hair follicle phenotypes (A and B) RNA in situ hybridization (A) and immunofluorescense (B) of Lrig1 in adult mouse dorsal skin (P45). Skin tissue sections were counterstained with DAPI to label nuclei (blue). (C) Schematic representation of the genetic

elements for Lrig1 lineage tracing during adult homeostasis and the experimental setup. (D) Dorsal skin tissues of Lrig1-CreERT2/Rosa26-mTmG mice collected 2 days, 5days, 1 week, 2 weeks and 4 weeks after 4-OHT treatment at P45, counterstained with DAPI to label nuclei (blue), red fluorescence of membrane tdTomato was not shown. JZ, junctional zone; INF, infundibulum; SG, sebaceous gland; SGbasal, basal cells of sebaceous gland; sebo, differentiated sebocytes. Scale bars, 50 μm. (E and F) Schematic representation of the genetic elements for Apc deletion (E) and Ctnnb1 deletion (F) and experimental setups. (G) H&E stained sections of dorsal skin from Lrig1-Apc mutant and control mice (APC Ctrl) 7 days and 11 days after 4-OHT treatment. (H) H&E stained sections of dorsal skin from Lrig1-βcat mutant and control mice (βcat Ctrl) 2 weeks and 4 weeks after 4-OHT treatment. (I and J) Quantifications of infundibulum/junctional zone dimensions and the sebaceous glands volumes (indicated by lipidTOX staining in green). Length, measurement from IFE to the point of SG duct connecting to the HFs; Width (lower), thickness of cell layers in the junctional zone; Width (upper), thickness of the cell layers in the infundibulum; Width (max), maximum diameters of the JZ cysts. N=60-180 imaged hair follicles from 2-5 mice in each group, respectively. N=110-290 sebaceous glands from 2-5 mice. Data are mean±SEM. ***p<0.001. (K) Schematic of phenotype development in Lrig1-Apc (11 days) and Lrig1-βcat (4 weeks) mutants.

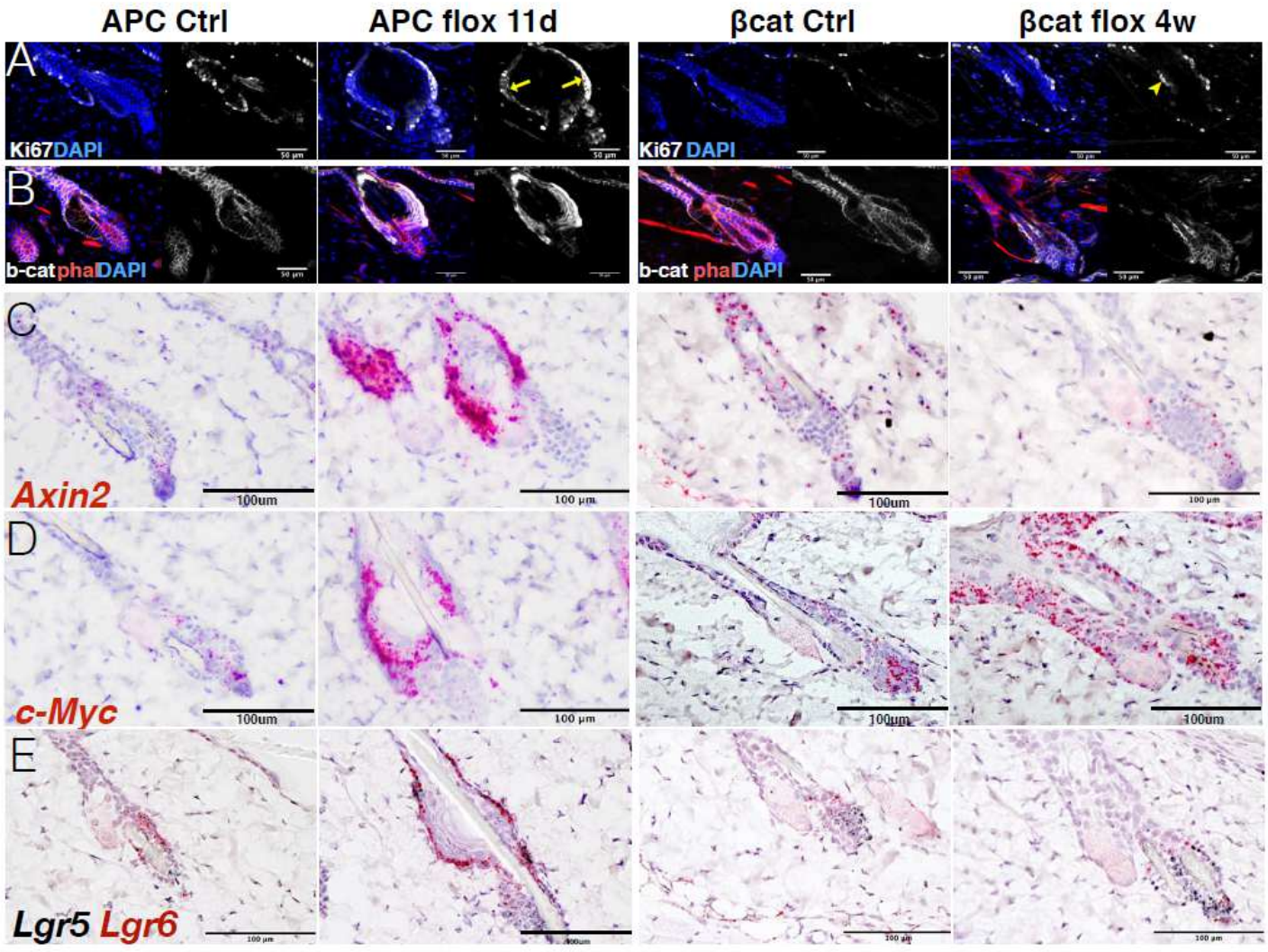

Figure 2

Wnt-hyperactivated JZ cysts contain large numbers of cells expressing Lgr6 and Lgr5 (A and B) Immunolabeled with the Ki-67 (A) and b-catenin (B) antibodies, and counterstained with phalloidin to label F-actin (red) or with DAPI to label nuclei (blue). Single color images for β-catenin and Ki-67 are shown in gray scale. Arrows and arrowhead indicate Ki67+ve cells in Lrig1-Apc cyst and Lrig1- βcat JZ, respectively. Scale bars, 50 μm.(C-E) Representative images of RNA in situ hybridization for Wnt targeted genes: Axin2 (C), c-Myc (D), Lgr6 and Lgr5 (E) as performed on Lrig1-Apc and Lrig1- βcat mutants and controls. Scale bars, 100 μm.

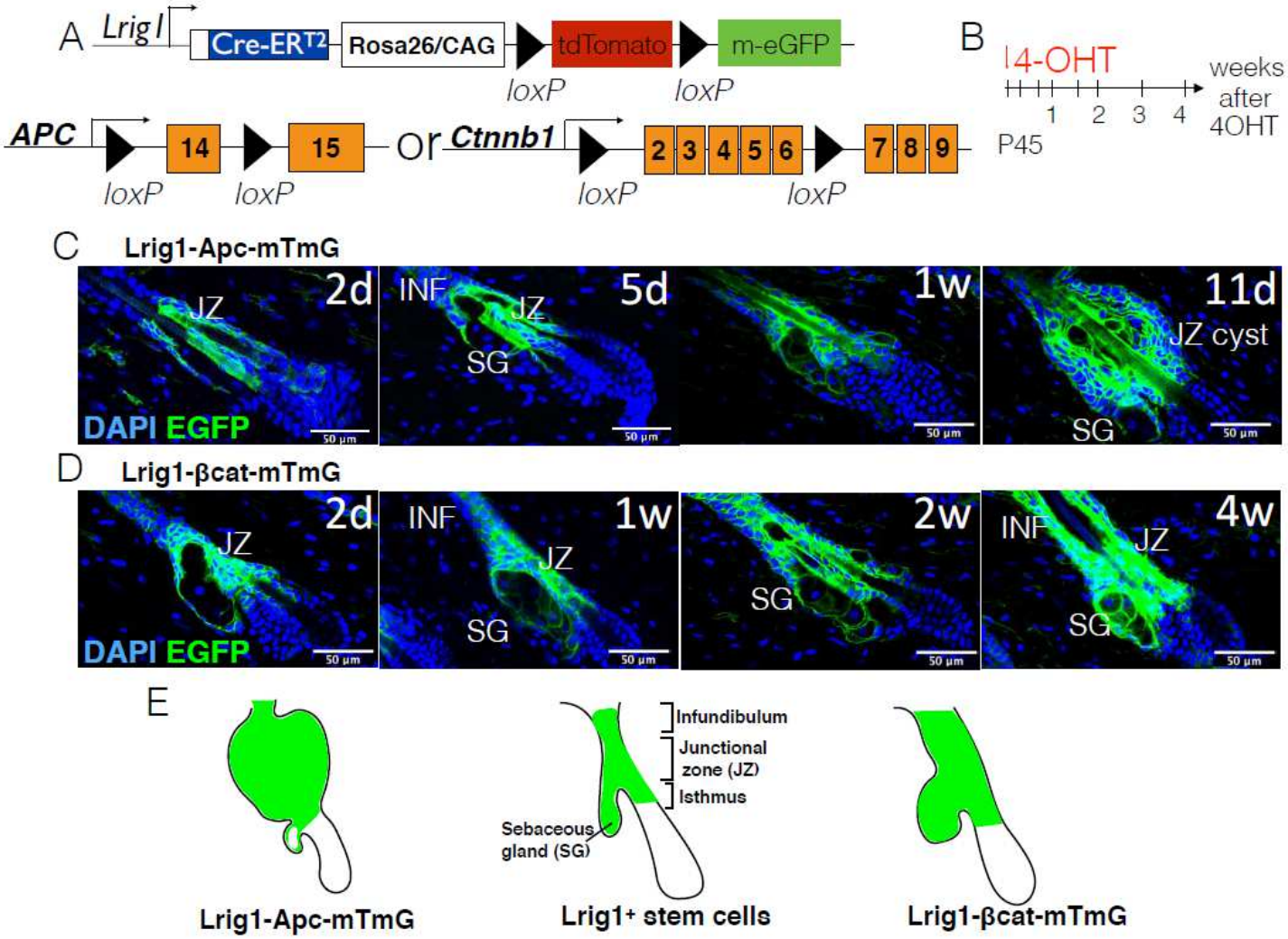

Figure 3

Contributions of Lrig1+ve stem cells when Apc or Ctnnb1 was deleted (A and B) Schematic representation of the genetic elements for lineage tracing (A) and experimental setups (B). (C and D) Dorsal skins collected at serial time points as indicated after 4-OHT treatment and stained with DAPI. Red fluorescence of membrane tdTomato was not shown. Scale bars, 50 μm. (E) Schematic of Lrig1+ve stem cells contributions to upper HFs when Apc or Ctnnb1 was ablated.

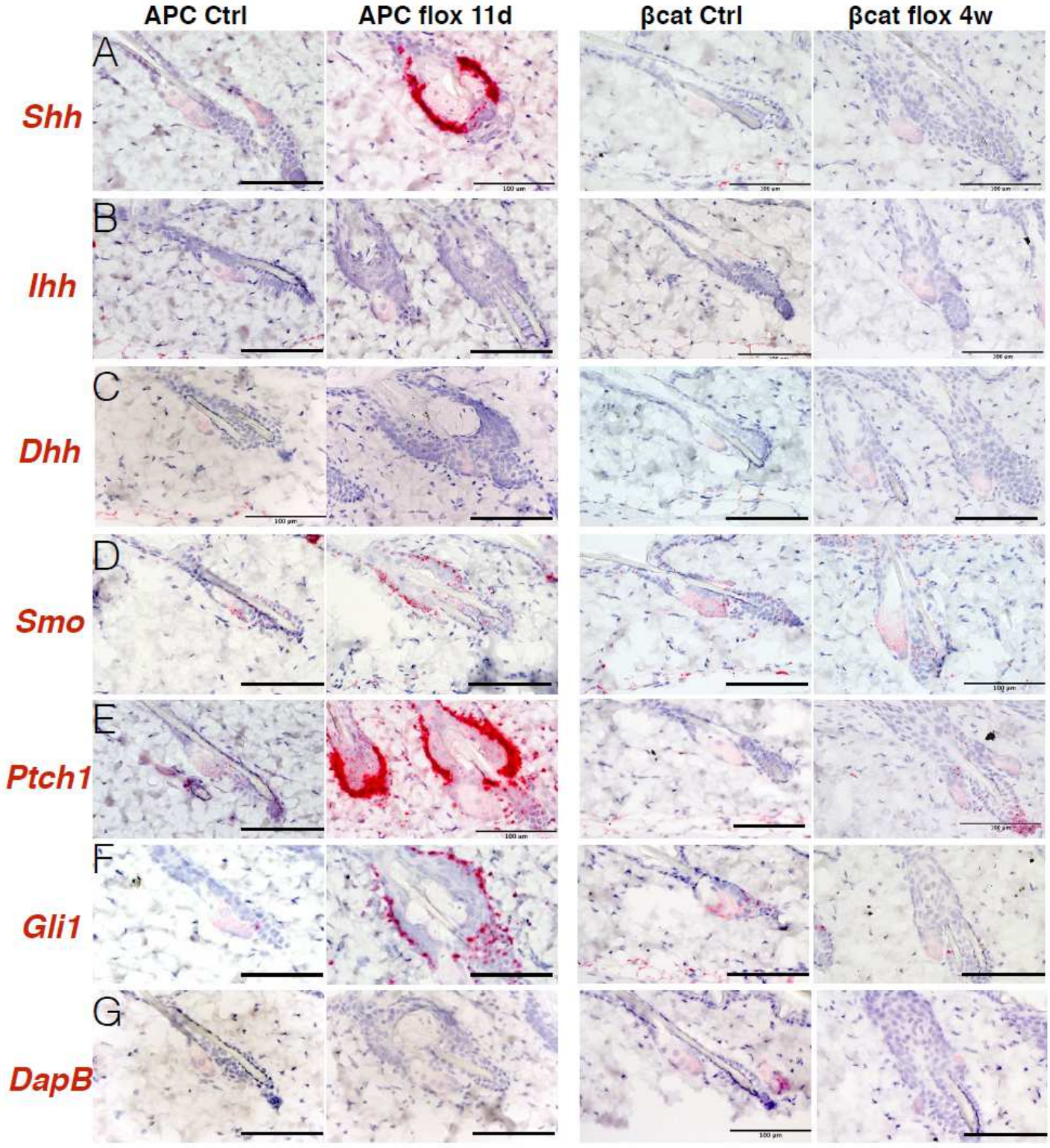

Figure 4

Hedgehog signalling was upregulated in APC loss/Wnt activation induced JZ cyst, but not Ctnnb1 loss-induced expansions (A-G) RNA in situ hybridization of genes in Hedgehog signaling pathways in Lrig1-Apc (11 days) and Lrig1-βcat cat (4 weeks) mutants and controls. Shh, Sonic hedgehog; Ihh, Indian hedgehog; Dhh, Desert hedgehog; Smo, smoothened; DapB, negative control. Scale bars, 100μm.

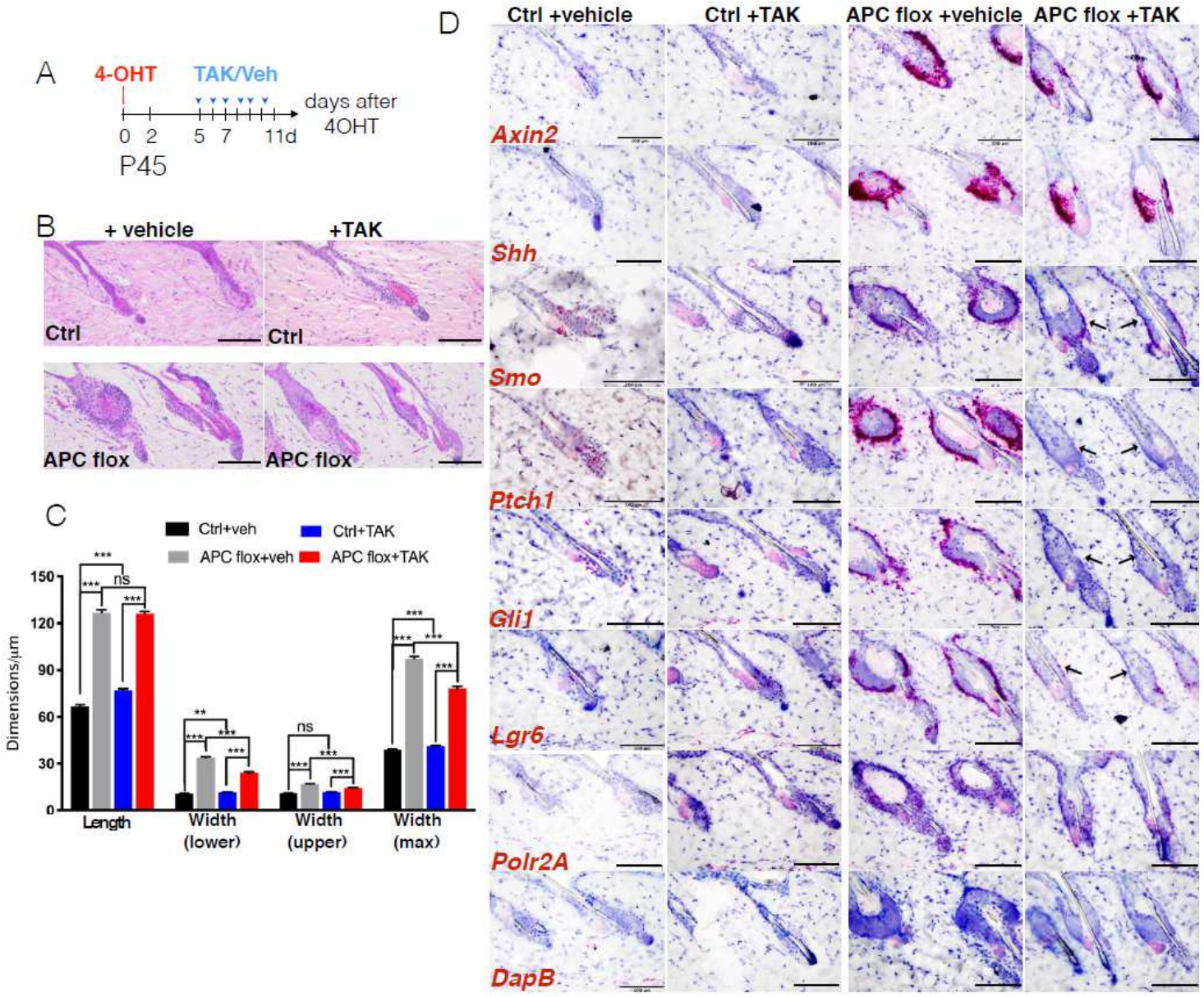

Figure 5

APC loss/Wnt activation induced cyst formation is Hedgehog signaling-dependent. (A) Experimental setup. Mice were topically treated with 4-OHT at P45 and subsequently with 1% TAK- 441 single dose daily from P50 till tissue harvest. (B) H&E staining of dorsal skin sections from Lrig1-Apc mutant and controls treated with vehicles or TAK-441. Scale bars, 50µm. (C) Quantifications of infundibulum/junctional zone dimensions and the sebaceous glands volumes of Lrig1-Apc mutant and controls treated with vehicles or TAK-441. N=153-184 imaged hair follicles from 2-3 mice in each group, respectively. Data are mean±SEM. ***p<0.001. (D) RNA in situ hybridization of Axin2, Shh, Smoothened, Ptch1, Gli1 and Lgr6 in Lrig1-Apc mutant and controls treated with vehicles or TAK-441. DapB, negative control; Polr2A, positive control. Scale bars, 100 µm.

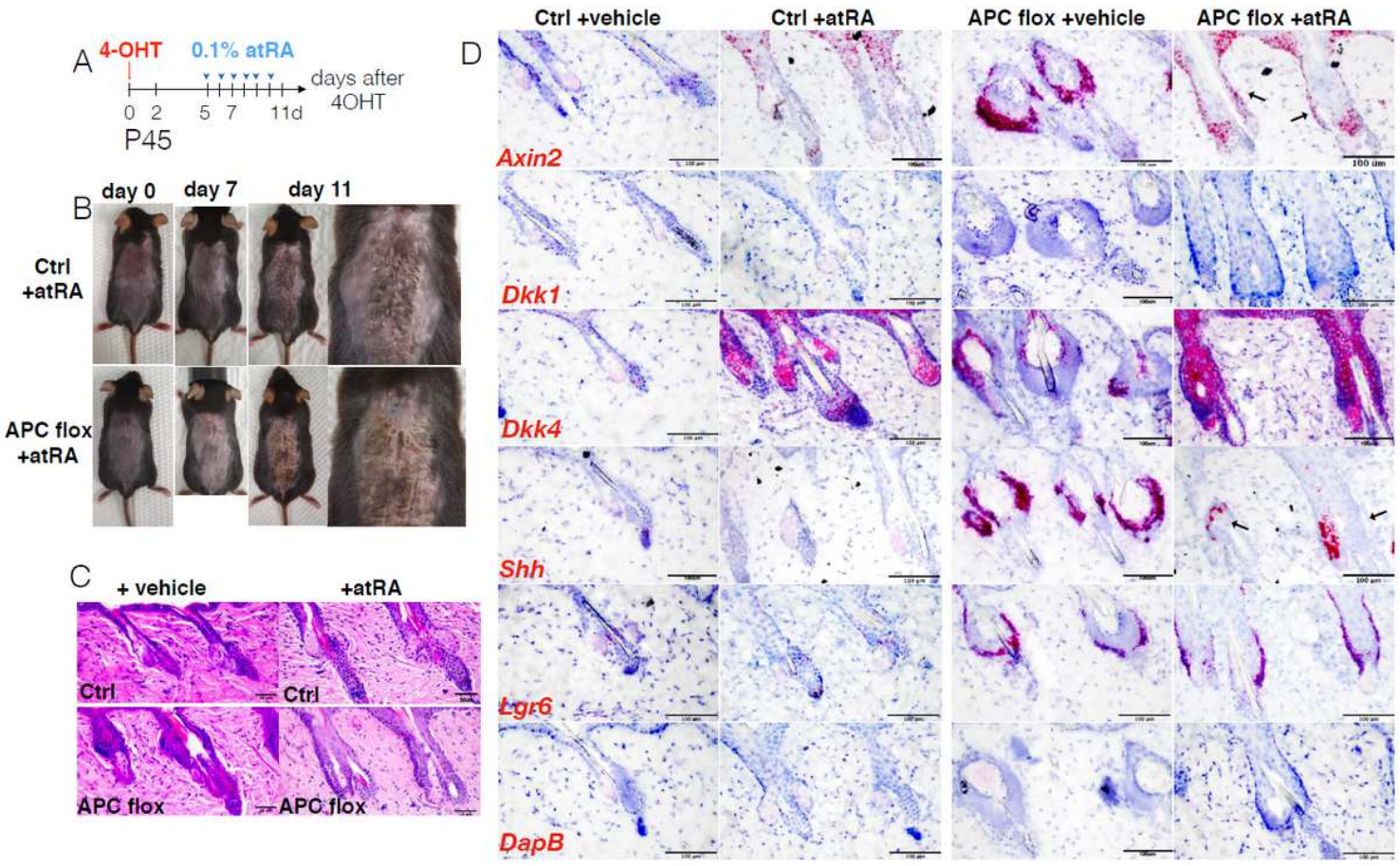

Figure 6

All-trans Retinoic acid rescued Lrig1-Apc mice phenotypes (A) Experimental setup. Mice were topically treated with 4-OHT at P45 and subsequently with 0.1% all-trans-Retinoic acid (atRA) single dose daily from P50 till tissue harvest. (B) Representative pictures of shaved and treated Lrig1-Apc mutant and control mice skin changes with 0.1% atRA applications.(C) H&E staining of dorsal skin sections from Lrig1-Apc mutant and controls treated with vehicles or atRA. Scale bars, 50μm. (D) RNA in situ hybridization of Axin2, Dkk1, Dkk4, Shh, Lgr6 and DapB in Lrig1-Apc mutant and controls treated with vehicles or atRA. Scale bars, 100 μm.

Supplementary Files

This is a list of supplementary files associated with this preprint. Click to download.

- SupplementaryFigures.pdf